Published in final edited form as:
J Struct Biol. 2010 July ; 171(1): 102–110. doi:10.1016/j.jsb.2010.02.018.

Automated Electron Microscopy for Evaluating Two-dimensional Crystallization of Membrane Proteins

Minghui Hu[a], **Martin Vink**[a,b], **Changki Kim**[a], **KD Derr**[a], **John Koss**[c], **Kevin D'Amico**[c], **Anchi Cheng**[d], **James Pulokas**[d], **Iban Ubarretxena-Belandia**[b], and **David Stokes**[a,e,f]

[a] New York Structural Biology Center, 89 Convent Ave., New York, NY 10027

[b] Dept. of Structural and Chemical Biology, Mt. Sinai School of Medicine, 1425 Madison Ave., New York, NY 10029

[c] JKD Instruments, LLC, 720 West Walnut St., Hinsdale, IL 60521

[d] The National Resource for Automated Molecular Microscopy, Dept. of Cell Biology, The Scripps Research Inst. 10550 North Torrey Pines Road, CB-129, La Jolla, CA 92037

[e] Skirball Institute and Dept. of Cell Biology, NYU School of Medicine, 540 First Ave., New York, NY 10016

Abstract

Membrane proteins fulfill many important roles in the cell and represent the target for a large number of therapeutic drugs. Although structure determination of membrane proteins has become a major priority, it has proven to be technically challenging. Electron microscopy of two-dimensional (2D) crystals has the advantage of visualizing membrane proteins in their natural lipidic environment, but has been underutilized in recent structural genomics efforts. To improve the general applicability of electron crystallography, high-throughput methods are needed for screening large numbers of conditions for 2D crystallization, thereby increasing the chances of obtaining well ordered crystals and thus achieving atomic resolution. Previous reports describe devices for growing 2D crystals on a 96-well format. The current report describes a system for automated imaging of these screens with an electron microscope. Samples are inserted with a two-part robot: a SCARA robot for loading samples into the microscope holder, and a Cartesian robot for placing the holder into the electron microscope. A standard JEOL 1230 electron microscope was used, though a new tip was designed for the holder and a toggle switch controlling the airlock was rewired to allow robot control. A computer program for controlling the robots was integrated with the Leginon program, which provides a module for automated imaging of individual samples. The resulting images are uploaded into the Sesame laboratory information management system database where they are associated with other data relevant to the crystallization screen.

[f] Corresponding author: stokes@nyu.edu, tel: 1-212-263-1580, fax: 1-646-219-0300.

Video 1. Robotic specimen insertion. The first part of the video shows the SCARA robot loading an EM grid into the sample holder. The second part of the video shows the Cartesian robot transferring the sample holder into the EM. The ~30 s required for pumping the airlock prior to insertion of the holder into the goniometer has been significantly abbreviated. Removal of the holder and the EM grid are essentially the reverse of these movements.

Keywords

automation; crystallography; electron microscopy; membrane protein; protein structure; structural genomics; two-dimensional crystal

1. Introduction

Automation is increasingly wide-spread, in scientific research, in manufacturing and in everyday life. Automation improves throughput and reproducibility of a well-defined task, both of which have proven essential for a variety of biological and industrial applications. For example, X-ray crystallographers increasingly rely on automation for crystallization trials and, more recently, for data collection [1]. The corresponding increase in throughput has facilitated their success with increasingly complex systems and, in particular, with membrane proteins which require more extensive screening and generally produce more poorly ordered crystals [2]. A screen of 10,000 conditions would be impractical using 24-well plates set up manually even by the most ambitious postdoc. The task of sorting through 200 individual crystals at the synchrotron to find the one that diffracts to high resolution would not be possible without a sample loading robot. For these reasons, efforts in automation and miniaturization are critical to the research centers involved in the NIH Protein Structure Initiative [3].

Electron crystallography is a method of structure determination that uses electron microscopy (EM) to image two-dimensional (2D) crystals [4]. This method is especially attractive for membrane proteins, which can be visualized in the natural environment of a lipid membrane. Electron crystallography has on a number of occasions resulted in atomic resolution structures [5], but like X-ray crystallography there is a significant bottleneck in producing suitable crystals. Methods for automating 2D crystallization would facilitate the exploration of the broad range of experimental parameters known to affect crystal formation: e.g., pH, salt, temperature, detergent, lipid composition and lipid-to-protein ratio of the reconstituted membrane [6]. Furthermore, automation would improve reproducibility of crystallization, which is critical for electron crystallography due to the large number of crystal images that contribute to a 3D dataset. Because 2D crystals are very thin (~5nm) and relatively small (~10μm), electron microscopy must be used both to evaluate the screens and to collect the data. For each crystallization condition, an aliquot must be applied to a carbon-coated EM grid followed by multiple drops of negative stain. After blotting and drying, grids are individually loaded into a specimen holder, inserted into the EM, searched at low magnification to locate putative crystals and finally imaged at higher magnification to evaluate their size and quality. When done manually, this labor-intensive process represents another significant bottleneck that hinders the application of 2D electron crystallography on a routine basis. We have recently described an automated approach for conducting 2D crystallization with a 96-well dialysis block and for producing negatively stained samples in parallel using a liquid-handling robot [7;8]. In this follow-up report, we describe our solution for automated imaging of these samples by electron microscopy.

Since the introduction of computer control in the late 1980's, electron microscopy has relied increasingly on automation. Electron tomography and focused ion beam milling are two applications that are not practical without computer control. A variety of software packages have been developed to automate collection either of standard projection images [9-13] or of an image tilt series suitable for tomographic reconstruction [14-17]. The Leginon imaging program goes further by providing an expandable set of EM operations that can be combined to automate a variety of applications. Currently, the Leginon software includes built-in applications designed for imaging single particles [18], for screening crystallization

trials [19], and for tomography [20]. The single particle application is the most advanced and a pipeline has been developed that feeds images directly from the image acquisition programs into a 3D reconstruction engine [21]. Such pipelines are proving highly effective for collecting large datasets from well characterized samples of isolated macromolecules, thus facilitating 3D reconstruction by single particle analysis.

For screening crystallization conditions, a large number of different EM grids must be screened and two approaches for automated sample insertion have been described. Potter et al. developed an articulated robot for loading individual grids into the sample holder and inserting them into the microscope [22]. The Leginon software was used to coordinate robotic insertion and to record images from the individual grids. Alternatively, Lefman et al. collaborated with a commercial vendor (Gatan Inc., Pleasanton CA) to develop a cartridge-based specimen holder, the “Gatling gun”, that simultaneously holds 100 EM grids within a pre-pumped specimen chamber attached to the microscope [23]. Clipping of EM grids into the cartridges and loading of cartridges into the cylindrical holder are both manual operations. After transferring this holder into the microscope, a script for the Gatan CCD imaging software (DigitalMicrograph) orchestrates sample insertion and imaging. Although both of these systems show promise for the screening of 2D crystallization trials, they are not widely used in the field. In the current report, we describe the design and implementation of a two-stage robot for loading samples into a JEOL1230 electron microscope as well as our adaptation of the Leginon software to control sample loading and imaging. This system represents a robust framework with which to screen conditions for producing 2D crystals, thus enabling electron crystallography to become a more effective technique for structure determination of membrane proteins.

2. Overall design of system

Our automated grid-loading and imaging system is schematically represented in Fig. 1, and consists of three parts: (1) the JEOL 1230 transmission EM, (2) the robotics responsible for insertion/removal of the specimen into/out of the microscope, and (3) software that coordinates robotic activities and that acquires images from each sample. Sample insertion/removal is broken into two steps that are handled by a SCARA robot and a Cartesian robot, respectively. Specifically, the SCARA-robot, transfers EM grids from a 96-well grid tray to the tip of the sample holder and the Cartesian robot picks up the holder and transfers it into the microscope. As can be seen in Video 1, these robots are located behind and to the right of the microscope console, leaving space in front of the microscope for manual use by an operator. For safety, a STOP button is prominently located next to the microscope console, which stops all robotic movement in an emergency.

The control software also consists of two components. The Leginon software package provides the interface with the electron microscope and a python program called iRobot controls movement of the SCARA and Cartesian robots. Leginon includes a large number of different python modules, which are linked together to automate a variety of EM applications [11;18]. One of these modules controls robotic specimen insertion and has been linked with other modules for analyzing the sample and collecting images at a number of different magnifications, thus providing a platform for screening a series of EM grids [22]. Leginon communicates with iRobot via a database, which contains calibrations, imaging parameters, images and the status of ongoing operations, thus requesting insertion or removal of a specific EM grid.

3. Hardware System

3.1. Grid handling

A Yamaha YK250X SCARA robot is employed for loading EM grids from a 96-well tray into the sample holder (Fig. 2). The robot has four motors, three of which generate rotation about the vertical (z) axis and one of which generates linear movement along this axis. The rotational movements are combined to generate linear movement of the grid handling probe in the x-y plane, which is used to move between the grid tray and the sample holder. The precision of these movements are ±0.01mm for translation and ±0.01° for rotation. The SCARA robot has a small footprint (~4000 cm^2) and is mounted on a table ~1 m above and behind the microscope console. This table also accommodates the EM sample holder and the 96-well EM grid tray, which are both within the limited range of motion afforded by the SCARA robot design.

The EM grid tray (Fig. 2c) was designed with standard SBS dimensions with 96-wells that are 0.9mm deep and 3.1mm in diameter. This diameter is only slightly larger than the standard EM grid (3.05mm), thus ensuring that the grids remain centered. The trays have an overall height of 10mm and were manufactured from aluminum using a programmable CNC mill and were black anodized. Since the trays are relatively inexpensive, many copies were made to allow storage of screens for potential reevaluation at a later date. The trays are securely held by a spring-loaded clamp to ensure that they are precisely positioned relative to the SCARA robot.

Different probes were evaluated for transferring grids from the storage tray to the sample holder. Forceps are commonly used for manual manipulation of EM grids, but were rejected as difficult to implement for a robot probe. As an alternative, we designed a vacuum probe consisting of three nozzles that are mounted vertically at the tip of the robot arm (Fig. 2b). The nozzles have an inner and outer diameter of 0.25 and 0.5mm, respectively and contact the rim at the perimeter of the grid, thus minimizing damage to the carbon film. The vacuum was generated using the Bernoulli effect, for which we used oil-free compressed air to feed a vacuum valve (Anver Corp, Hudson MA) that was mounted under the robot stand and connected to the nozzles through tygon tubing. Suction is turned on by simply applying voltage to the valve and the resulting vacuum pressure was controlled by the input pressure (60 psi) to optimize grid pickup. We found that this configuration minimizes grid deformation that might otherwise cause mishandling or misplacement of individual grids. A single nozzle was also effective in lifting the grids but, if applied to the center of the grid, it routinely damaged the carbon film and, if applied to the rim, the grids tended to rotate thus becoming incorrectly positioned for release onto the holder. Commercial rubber suction cups were also evaluated, but these tended to generate static electricity and furthermore contacted a large region of the grid, potentially causing widespread damage to the carbon film. Using the vacuum probe, the SCARA robot has a 98% success rate in transferring grids to the holder. The remaining 2% never get picked up from the grid tray, presumably due to grid deformation. The nozzle occasionally becomes magnetized and therefore fails to release the grids onto the holder, a situation which is quickly remedied with a demagnetizer.

3.2. Sample holder

The tip of the standard EM sample holder was redesigned to accommodate operation by the SCARA robot (Fig. 3). In particular, loading an EM grid into the high stability holders from JEOL requires manipulation of a delicate arm that is held in place by multiple fine screws. The standard holder for the JEOL 1230 microscope features a quick-change clamp that must be pulled down with significant force to either secure or release the grid. The unclamping is unpredictable and sometimes leads to the EM grid jumping out of position or out of the

holder all together; once released, the clamp has considerable side-to-side play and is highly mobile. Fortunately, the entire tip is fastened to the arm of the sample holder by three screws and can be readily exchanged with alternative tips.

The new tip was milled from brass and equipped with a spring-loaded cam that can be raised and lowered in a controlled way (Fig. 3b). This clamp has a 90° range of motion, from vertical (open) to horizontal (closed), with very little side-to-side play. The distal end of the clamp - furthest from the handle - extends beyond the end of the tip by 5mm, thus providing a handle for raising and lowering the clamp. This extension is engaged by an L-shaped finger attached to the probe of the SCARA robot next to the vacuum nozzle (Fig. 3c,e). The cam-shaped hinge is loaded with a spring such that it comes to rest at either the fully open or fully closed position and applies pressure that holds the grid firmly in place.

To ensure a reproducible position of the EM sample holder relative to the two robots, a custom-made mount was constructed (Fig. 3a). A precise orientation of the holder is maintained by a pin on the mount that inserts into a hole milled into the bottom of the holder handle.

In an attempt to verify the presence of an EM grid both in the 96-well tray and in the sample holder during transfer by the SCARA robot, a small laser was mounted on the robot probe. However, the reflected signal from the Ni-grids proved to be unreliable, due both to lack of flatness and to discoloration from carbon coating and sample staining. Instead, we decided to rely on the initial low magnification images from the EM to determine if a grid had been successfully loaded into the holder. Given the high success rate of the SCARA robot in transferring grids, this is a rare event. Once the clamp has been lowered, the grids remain securely fastened and we have not experienced any loss during transfer of the holder into the microscope.

3.3. Sample Insertion

Once the SCARA robot loads an EM grid onto the tip of the sample holder, a four-axis Yamaha MXY-x Cartesian robot picks up the holder and transfers it to the electron microscope (Fig. 4). A pneumatic, three-fingered gripper (P5G-HPC-320, Parker Hannifin Corp, Cleveland OH) is used to grasp the handle of the specimen holder (Fig. 4b). The Cartesian robot then carries the holder to the entrance of the airlock using three motors to generate linear movements along the x, y, and z axes. These motors have adjustable torque, a maximum speed of 1200mm/s, and an accuracy of 0.01mm. The gripper is attached to a rotational motor, which enables manipulation of the holder through the airlock.

The maximum torque allowed for these four motors was restricted in order to minimize potential damage to the microscope as well as the consequences of accidental contact with foreign objects. Each motor was characterized by a minimal torque required to overcome its innate, internal resistance; lower torques produced chatter or resulted in no movement at all. After empirically establishing the threshold for each motor, the torque was increased slightly above this threshold to provide reliable movement. Rotation through the airlock and removal of the holder from the column required somewhat higher torque than other movements, but in all cases motion can be easily stopped using one or two fingers (i.e., <5N of force). The iRobot program monitors each movement and if the endpoint does not correspond to the expected position, then it assumes that some impediment has been encountered and all further movements are immediately halted.

Alignment of the Cartesian robot with the axis of the microscope goniometer is critical. Improper alignment can result in damage to the microscope or to the holder, especially during rotation in the airlock. Specifically, a guide pin on the holder engages a groove on the

airlock, thus opening relevant valves and gaining access to the column. As a first step in the alignment process, the Cartesian robot was mounted such that its axis of insertion was roughly parallel to the goniometer axis. However, mechanical failure of an optical switch operated by the guide pin alerted us to an angular misalignment between the insertion angle of the Cartesian robot and the goniometer. Unfortunately, neither the linear x-y-z motors nor the on-axis rotation stage allowed adjustment of the entrance angle. Nevertheless, the goniometer itself provided a mechanism for adjusting its axis of insertion relative to the robot. Specifically, translation of the EM grid inside the microscope along y and z axes is effected not by linear motions, but by slight rotations of the holder (the x axis corresponds to the rod axis and z is vertical). The pivot point for these rotations is relatively close to the EM grid, such that a small (1 mm) translation of the grid results in a much larger (5 mm) movement of the handle. Thus, moving the holder in the microscope in y and z produced different angles of the sample rod relative to the fixed coordinate system of the robot. The y axis has a larger range and required more adjustment than the z axis, since both the goniometer and the robot were mounted close to level. Translation along the rod axis (x) is in fact linear and therefore does not affect the entrance angle.

To establish an optimal alignment, the sample holder was inserted into the microscope and the unclenched grippers were positioned around the handle. The run-out was then measured as the grippers were rotated around the handle. If necessary, the holder was moved within the goniometer to a new position (i.e., a different angle) and the Cartesian robot was translated to the new position adopted by the handle. This procedure was iterated until an optimal goniometer “home” position was established, where axis of the Cartesian robot was parallel to the entrance cylinder of the goniometer. During this process, we found that the axis of the rotation stage on the Cartesian robot needed adjustment to be precisely parallel to the direction of insertion, since the robot specifications were rather lax in this regard. Also, in order to maintain the accuracy of the holder orientation, we replaced the original hollow, plastic handle of the EM holder with a solid aluminum handle, thus preventing deformation of the original hollow plastic handle by the gripper. Although the diameter of this handle was arbitrary, it was important to ensure that it was concentric with the sample holder rod and tip, so that rotations in the airlock did not give rise to displacements of the sample holder rod. Overall, we estimate a margin of error for this alignment to be about ±0.5mm. All these considerations are moot when it comes to manual insertion, because an operator does not rigidly grip the holder at a specific location or angle relative to the goniometer.

The reproducibility of this alignment requires that the microscope remain in a defined position relative to the robot. The routine use of anti-vibration mounts for electron microscopes is a potential problem in this regard, especially with air mounts that allow substantial column movement and have the potential to get out of balance, e.g., due to dirty air valves. The rubber mounts employed by the JEOL 1230 are much stiffer and appear so far to return the column to a reproducible position. However, we mounted a single small laser onto the microscope column and marked the position of its beam on the wall of the room to provide a long-term, visual monitor of the position of the column. If column movement were to become a problem, one could mount a laser on the probe and an optical sensor on the microscope; a feedback system could then be established to help the Cartesian robot home in on the optimal position prior to insertion of the holder. With very compliant anti-vibration mounts, it is conceivable that the force of insertion/removal would push the column out of alignment, in which case it would be advisable to take measures to stiffen the mounts or minimize the force used for insertion and removal.

4. Software System

iRobot is a python program that we developed to orchestrate the movements of the SCARA and Cartesian robots. iRobot runs on a dedicated Linux computer and communicates directly with IP-enabled controllers associated with each of the robots; these controllers store the coordinates as well as the speed and torque for each designated movement (Fig. 5). These coordinates are established and, if necessary, readjusted by manually moving each robot to points along its route, using either a hand-held control panel or a custom module in the iRobot program; the latter provides a somewhat safer, more convenient way to control the robots and is useful in recovering from problems. For calibrating the coordinates of each well in the grid tray, the SCARA robot was manually positioned at each of the four corner wells and the positions of the remaining 92 wells were calculated based on their center-to-center spacing. iRobot is also equipped with module for manually inserting and removing a sample, which is helpful for novice EM users and for testing robot performance. During operation, iRobot monitors the vacuum in the microscope airlock, thus inserting the specimen only after the airlock has been pumped to a sufficiently low vacuum and removing the specimen only after this airlock has been vented to air. In order to measure the vacuum on the JEOL 1230, a wire was run from a vacuum test point on the microscope to an analogue-to-digital board on the robot control computer. Also, a modification was necessary to the toggle switch that controls whether the airlock is in the pump or vent state, which are required for insertion and removal, respectively. This switch was rewired so that this toggle switch can be bypassed and iRobot can control the state of the airlock using a relay. A secondary toggle switch was put in-line either to establish this bypass or to allow normal manual operation. Currently, the JEOL1230 is fitted with a tungsten filament, which is turned off during specimen exchanges; however, the double O-ring design of the JEOL holder lowers the chance of a vacuum leak through the airlock, thus allowing for the use of the longer-lived LaB_6 filament in the future.

Leginon is also developed in python and is distributed by NRAMM with a number of modular tasks that are logically strung together into “applications”, e.g. for imaging single particles and for tomography [18]. Information about the microscope, the CCD camera, the sample and the desired operating conditions is stored in a MySQL database, which resides on a separate computer and which is available not only to the various modules, but also to external programs that wish to query this database. NRAMM previously developed modules both for managing robotic sample insertion and for screening EM grids, which represented a starting point for our application. Nevertheless, certain modifications were necessary given the different communication protocol used by the JEOL 1230 microscope and the requirements of our robot control software.

Leginon uses the pyScope library to communicate with a range of different microscopes and CCD cameras, which include Tecnai and CM microscopes from FEI microscopes as well as microscopes using the TEMCOM interface from JEOL [18]. We developed a new module called Jeol1230.py to implement the relevant command codes for the JEOL 1230. Specifically, commands for reading and setting magnification, brightness, focus, stage position, beam shift, etc. were obtained from the manufacturer and a python extension (pySerial) was used for RS-232C communications. A significant amount of testing was required to understand the operational constraints of the various commands and critical differences were identified relative to the FEI instruments. For example, there is no command to change the relative focus of the JEOL 1230, only a command to set the absolute level of current in the upper and lower objective lenses. Thus, objective lens values corresponding to eucentric focus were saved in a file and a new calibration procedure was developed to determine changes required to achieve a given offset. Also, movement of the JEOL 1230 goniometer includes a parameter to control the speed, but exhibited a threshold,

below which it did not move at all. Like FEI microscopes, accurate stage positioning requires a backlash correction even when the holder was slowed down as it approached the desired position.

Previous versions of Leginon included a module designed to coordinate robotic sample insertion with grid screening [22], but we modified the underlying communication to make it more generic. The previous implementation included signals sent directly from Leginon to the particular robot in use, similar to the strategy adopted for the EM and the CCD camera. Our new implementation includes a new base class (Robot2) that registers a request for insertion in the MySQL database. In particular, to request insertion of a given grid from the 96-well tray, the Leginon robot module turns off the beam, sets the goniometer to the home position, and sets a logical field in the database table. Upon detecting this condition, iRobot initiates the insertion process. Once successfully completed, iRobot sets a companion logical field and Leginon then proceeds with the screening process. A similar handshaking is used to remove the sample.

For imaging individual samples, we used the Leginon 2D crystal screening application previously described by Cheng et al. [19] and depicted in Fig. 6. Specifically, the Robot MSI-Screen 1st Pass module was employed to record images at several different magnifications from widely distributed locations on a negatively stained grid. Images were recorded with a 1k × 1k CCD camera mounted in the 35mm port on the microscope (Gatan Erlangshen). For this process, imaging conditions at three different magnifications were defined, low magnification or grid-scale (gr) encompassing an ~250μm × 250μm area, intermediate or square-scale (sq) encompassing an area of ~50μm × 50μm, and high magnification or hole-scale (hl) encompassing an area of ~5μm × 5μm. Initially, a montage was assembled from a 3×3 array of grid-scale images (Fig. 6), which covered ~10% of the grid. The positions of individual grid squares were located within this montage using cross-correlation with a user-defined mask, which was simply a circle of approximately the same size as a grid square. Selected squares were chosen for further imaging based on density histograms. Images were then recorded at the square-scale after adjusting the Z-height of the grid to the eucentric position. A raster defined potential areas on each square-scale image for further imaging at the hole scale; again, the density histograms were used to select suitable areas. The goal was to take a relatively small number of images (<50) from various locations across the grid that provided an overview of the results of the crystallization condition. Although the hole-scale was not high enough magnification to evaluate crystal lattices, they were sufficient to characterize the overall morphology of the objects on the grid and to inform the operator whether a given grid was worthy of a closer look (Fig. 6). The Leginon 2D crystal screening module also includes a 2nd Pass module that is designed to re-image grids at higher magnification. Because the software is not currently able to select favorable objects for imaging, this process is very inefficient and remains an area for future development.

Leginon stores all these images to its MySQL database and provides a web-based, graphical interface for viewing them. However, in order to develop a pipeline for screening 2D crystallization, we require the images to be specifically associated with other information about the protein and about the conditions used for the crystallization screen. A Laboratory Information Management System (LIMS) known as Sesame, which was designed for laboratories involved in the Protein Structure Initiative (http://www.sesame.wisc.edu) [24] was therefore adopted. We have added features to associate images from the EM screen within the relevant crystallization conditions and added an image viewer to the graphical user interface (Fig. 7). Thus, results from our screen can be viewed and scored in the context of the Sesame relational database and thus used to guide our efforts in identifying and optimizing conditions for generating well ordered 2D crystals.

5. Discussion and future directions

Our overall aim is to develop a pipeline for solving the structure of membrane proteins by electron crystallography. The robots and associated software described above provide the back-end of this pipeline and complement the 96-well dialysis block and the 96-position staining platform that we have designed for high-throughput crystallization and preparation of EM grids [7;8]. Using this dialysis block, or an analogous crystallization device based on complexation of detergent by cyclodextrin [25], hundreds of EM grids can be readily generated on a weekly basis. At this rate, inspection of these grids becomes a significant bottleneck. When screened manually, 20-30 min are required to record 10-20 images that represent the various different kinds of objects on each grid. The nature of these objects is used to determine a score that characterizes the outcome of each crystallization condition. This is a tedious process that saps the energy and creativity of staff as well as detracting from the time spent on other aspects of the project. Thus, although the total cost of the robots was considerable (annual salaries for ~3 postdoctoral fellows), we believe that the long-term benefits of automation will ultimately make this a wise investment.

5.1.Choice of design

Previous reports have described alternative designs for robotic handling of EM samples. In particular, Potter et al. [22] employed an articulated robot to insert EM grids into a Tecnai F20 microscope. Our approach is similar in that grids are loaded one at a time through the airlock in a manner analogous to a manual operator. In this way, the microscope itself requires very few modifications. Unlike Potter et al., we adopted two robots instead of a single articulated robot, because the SCARA and Cartesian robots are generally easier to maintain and seldom require recalibration. A very different approach was adopted by Lefman et al. [23], who designed a so-called Gatling gun that accommodates 100 EM grids within the vacuum of a Tecnai T12 microscope. Similarly, the Engel laboratory has adapted FEI's “autoloader” unit for a Tecnai T12 microscope and interfaced it with a drum-like carousel holding eight Titan autoloader cassettes with 12 grids each (personal communication). For these last two systems, each grid must be manually loaded into a cartridge and then the cartridges must be mounted either directly onto a carousel or into the autoloader cassettes. In the case of the Gatling gun, the entire carousel resides inside the vacuum of the electron microscope, whereas the Tecnai T12 system transfers each 12-grid cassette from the carousel into the vacuum one at a time. After completing the screen, the carousel must be disassembled and the individual grids must be unmounted from the cassettes; if storage is desired, grids must be transferred to a separate device. Our design has the advantage of robotically loading grids into the sample holder as well as providing storage within the grid trays, thus allowing follow-up screens with a minimal amount of effort. Ultimately, these trays could be bar coded to further expand the scope of the operation. To control grid insertion and image collection, both Lefman et al. and the Engel laboratory have developed new software: a DigitalMicrograph script and an unnamed Matlab program, respectively. Like Potter et al. [22], we have used Leginon, which has the advantage of a broader base of supported microscopes and CCD cameras as well as a modular design that accommodates customization by individual users depending on their specific applications.

5.2. Efficiency of operation

The time required to screen each EM grid is close to 30 min, depending on the number of images recorded, which is comparable to manual screening. The whole process can be broken down as follows: 1 min to load an EM grid into the holder, 3 min to load the holder into the microscope, 2.5 min to initialize the microscope and to record a 3x3 montage at 400x magnification, 12 min to image nine selected grid squares at 2.5kx magnification and

to select areas suitable for imaging at higher magnification, 12 min to record a total of 25-30 images from these areas at 25kx magnification, 3 min to remove the holder and unload the EM grid. The mechanical steps of grid loading and unloading are minimal and not easily reduced. The time for selecting grid squares could potentially be reduced by faster movements of the goniometer, but this will impact accuracy and, in any case, the adjustment of eucentric height of each grid square takes considerably longer than the translation and cannot be significantly reduced.

In contrast, the efficiency in image collection can be potentially enhanced by introducing new target selection algorithms. Leginon currently relies on an analysis of density histograms and, as a result, is only moderately effective at identifying objects that are useful for evaluating a particular crystallization condition. Using an optimal density threshold on an EM grid with a good distribution of tubular crystals (e.g. Fig. 7), almost 90% of images (27 out of 31) included objects useful in scoring the crystallization condition. On a less optimal EM grid, less than 70% (17 out of 25) of images were useful, the others being mostly empty areas of the grid (e.g. Fig. 6d-f). Furthermore, these results are influenced by beam intensity, which tends to vary over long periods of time. An improved algorithm has been implemented that varies the density threshold based on statistical analysis of image densities across each grid square. Ultimately, we plan to develop shape recognition algorithms, which would allow a more intelligent selection of areas to image, thus making it worthwhile to include a higher magnification step capable of detecting crystal lattices.

Taking this one step further, shape recognition could also be used to assign a preliminary score to individual EM grids. Scoring currently relies on the judgment of a staff member, with crystals eliciting the highest score, aggregated protein or lipid the worst score, and non-crystalline proteoliposomes in between. Given the heterogeneity generally obtained on any given EM grid, the final score is an integration of all the objects identified. Automation of this process could allow researchers to focus on the most promising conditions. The Sesame LIMS is a natural place to implement automated scoring, since both the images and the scores are ultimately saved in this database and identification of important factors would involve correlation of results across a series of crystallization screens. Two-way communication between Sesame and Leginon is under development and will be used to move images into the Sesame database for evaluation. An analysis of these images would allow Sesame to direct Leginon to follow up with high magnification imaging of particularly promising samples. Once such a system is in place, we may be able to increase throughput by initially collecting a smaller number of hole-scale images for evaluation and then allow the scoring algorithm to determine whether it is worth spending additional time with that grid, or whether to move to the next.

Supplementary Material

Refer to Web version on PubMed Central for supplementary material.

Acknowledgments

The authors wish to acknowledge the help of Zsolt Zolnai in updating the Sesame LIMS for storage and display of EM images, Russ Hinchliffe for machining various pieces required for final robot implementation, JEOL engineers Rob Hynes and Robert Metzger for help interfacing the electron microscope to the robot and Ruben Diaz-Avalos for making the video of robot operations. Funding for this work was provided by NIH grant P41 RR17573 for development of Leginon, NIH grant R01 GM081817 and NSF grant MCB-0546087.

Abbreviations

CNC	Computer Numerical Control
CCD	Charge Coupled Device
EM	electron microscopy
LIMS	Laboratory Information Management System
NRAMM	National Resource for Automated Molecular Microscopy
SCARA	Selective Compliance Assembly Robot Arm
SBS	Structures for Bulk Solids
2D	two-dimensional
3D	three-dimensional

Bibliography

1. Sugahara M, Asada Y, Shimizu K, Yamamoto H, Lokanath NK, Mizutani H, Bagautdinov B, Matsuura Y, Taketa M, Kageyama Y, Ono N, Morikawa Y, Tanaka Y, Shimada H, Nakamoto T, Yamamoto M, Kunishima N. High-throughput crystallization-to-structure pipeline at RIKEN SPring-8 Center. J Struct Funct Genomics. 2008; 9:21–8. [PubMed: 18677553]
2. Wiener MC. A pedestrian guide to membrane protein crystallization. Methods. 2004; 34:364–72. [PubMed: 15325654]
3. Joachimiak A. High-throughput crystallography for structural genomics. Curr Opin Struct Biol. 2009; 19:573–84. [PubMed: 19765976]
4. Amos LA, Henderson R, Unwin PNT. Three-dimensional structure determination by electron microscopy of two-dimensional crystals. Prog. Biophys. Molec. Biol. 1982; 39:183–231. [PubMed: 6289376]
5. Hite RK, Raunser S, Walz T. Revival of electron crystallography. Curr Opin Struct Biol. 2007; 17:389–95. [PubMed: 17723294]
6. Jap BK, Zulauf M, Scheybani T, Hefti A, Baumeister W, Aebi U, Engel A. 2D crystallization: from art to science. Ultramicroscopy. 1992; 46:45–84. [PubMed: 1481277]
7. Vink M, Derr K, Love J, Stokes DL, Ubarretxena-Belandia I. A high-throughput strategy to screen 2D crystallization trials of membrane proteins. J. Struct. Biol. 2007; 160:295–304. [PubMed: 17951070]
8. Kim C, Vink M, Hu M, Stokes DL, Ubarretxena-Belandia I. An automated pipeline to screen membrane protein 2D crystallization. J. Func. Struc. Genomics submitted. 2010
9. Kisseberth N, Whittaker M, Weber D, Potter CS, Carragher B. emScope: A Tool Kit for Control and Automation of a Remote Electron Microscope. J. Struct. Biol. 1997; 120:309–319. [PubMed: 9441934]
10. Oostergetel GT, Keegstra W, Brisson A. Automation of specimen selection and data acquisition for protein crystallography. Ultramicroscopy. 1998; 74:47–50.
11. Potter CS, Chu H, Frey B, Green C, Kisseberth N, Madden TJ, Miller KL, Nahrstedt K, Pulokas J, Reilein A, Tcheng D, Weber D, Carragher B. Leginon: a system for fully automated acquisition of 1000 electron micrographs a day. Ultramicroscopy. 1999; 77:153–161. [PubMed: 10406132]
12. Zhang P, Beatty A, Milne JL, Subramaniam S. Automated data collection with a Tecnai 12 electron microscope: applications for molecular imaging by cryomicroscopy. J. Struct. Biol. 2001; 135:251–61. [PubMed: 11722165]
13. Zhang J, Nakamura N, Shimizu Y, Liang N, Liu X, Jakana J, Marsh MP, Booth CR, Shinkawa T, Nakata M, Chiu W. JADAS: a customizable automated data acquisition system and its application to ice-embedded single particles. J. Struct. Biol. 2009; 165:1–9. [PubMed: 18926912]
14. Koster AJ, Chen H, Sedat JW, Agard DA. Automated microscopy for electron tomography. Ultramicroscopy. 1992; 46:207–227. [PubMed: 1481272]

15. Zheng SQ, Keszthelyi B, Branlund E, Lyle JM, Braunfeld MB, Sedat JW, Agard DA. UCSF tomography: an integrated software suite for real-time electron microscopic tomographic data collection, alignment, and reconstruction. J. Struct. Biol. 2007; 157:138–47. [PubMed: 16904341]

16. Mastronarde DN. Automated electron microscope tomography using robust prediction of specimen movements. J. Struct. Biol. 2005; 152:36–51. [PubMed: 16182563]

17. Nickell S, Forster F, Linaroudis A, Net WD, Beck F, Hegerl R, Baumeister W, Plitzko JM. TOM software toolbox: acquisition and analysis for electron tomography. J. Struct. Biol. 2005; 149:227–34. [PubMed: 15721576]

18. Suloway C, Pulokas J, Fellmann D, Cheng A, Guerra F, Quispe J, Stagg S, Potter CS, Carragher B. Automated molecular microscopy: the new Leginon system. J. Struct. Biol. 2005; 151:41–60. [PubMed: 15890530]

19. Cheng A, Leung A, Fellmann D, Quispe J, Suloway C, Pulokas J, Abeyrathne PD, Lam JS, Carragher B, Potter CS. Towards automated screening of two-dimensional crystals. J. Struct. Biol. 2007; 160:324–31. [PubMed: 17977016]

20. Suloway C, Shi J, Cheng A, Pulokas J, Carragher B, Potter CS, Zheng SQ, Agard DA, Jensen GJ. Fully automated, sequential tilt-series acquisition with Leginon. J. Struct. Biol. 2009; 167:11–8. [PubMed: 19361558]

21. Lander GC, Stagg SM, Voss NR, Cheng A, Fellmann D, Pulokas J, Yoshioka C, Irving C, Mulder A, Lau PW, Lyumkis D, Potter CS, Carragher B. Appion: an integrated, database-driven pipeline to facilitate EM image processing. J. Struct. Biol. 2009; 166:95–102. [PubMed: 19263523]

22. Potter CS, Pulokas J, Smith P, Suloway C, Carragher B. Robotic grid loading system for a transmission electron microscope. J. Struct. Biol. 2004; 146:431–40. [PubMed: 15099584]

23. Lefman J, Morrison R, Subramaniam S. Automated 100-position specimen loader and image acquisition system for transmission electron microscopy. J. Struct. Biol. 2007; 158:318–26. [PubMed: 17240161]

24. Zolnai Z, Lee PT, Li J, Chapman MR, Newman CS, Phillips GN Jr. Rayment I, Ulrich EL, Volkman BF, Markley JL. Project management system for structural and functional proteomics: Sesame. J Struct Funct Genomics. 2003; 4:11–23. [PubMed: 12943363]

25. Iacovache I, Biasini M, Kowal J, Kukulski W, Chami M, Van der Goot FG, Engel A, Remigy HW. The 2DX robot: A membrane protein 2D crystallization Swiss Army knife. J. Struct. Biol. 2009

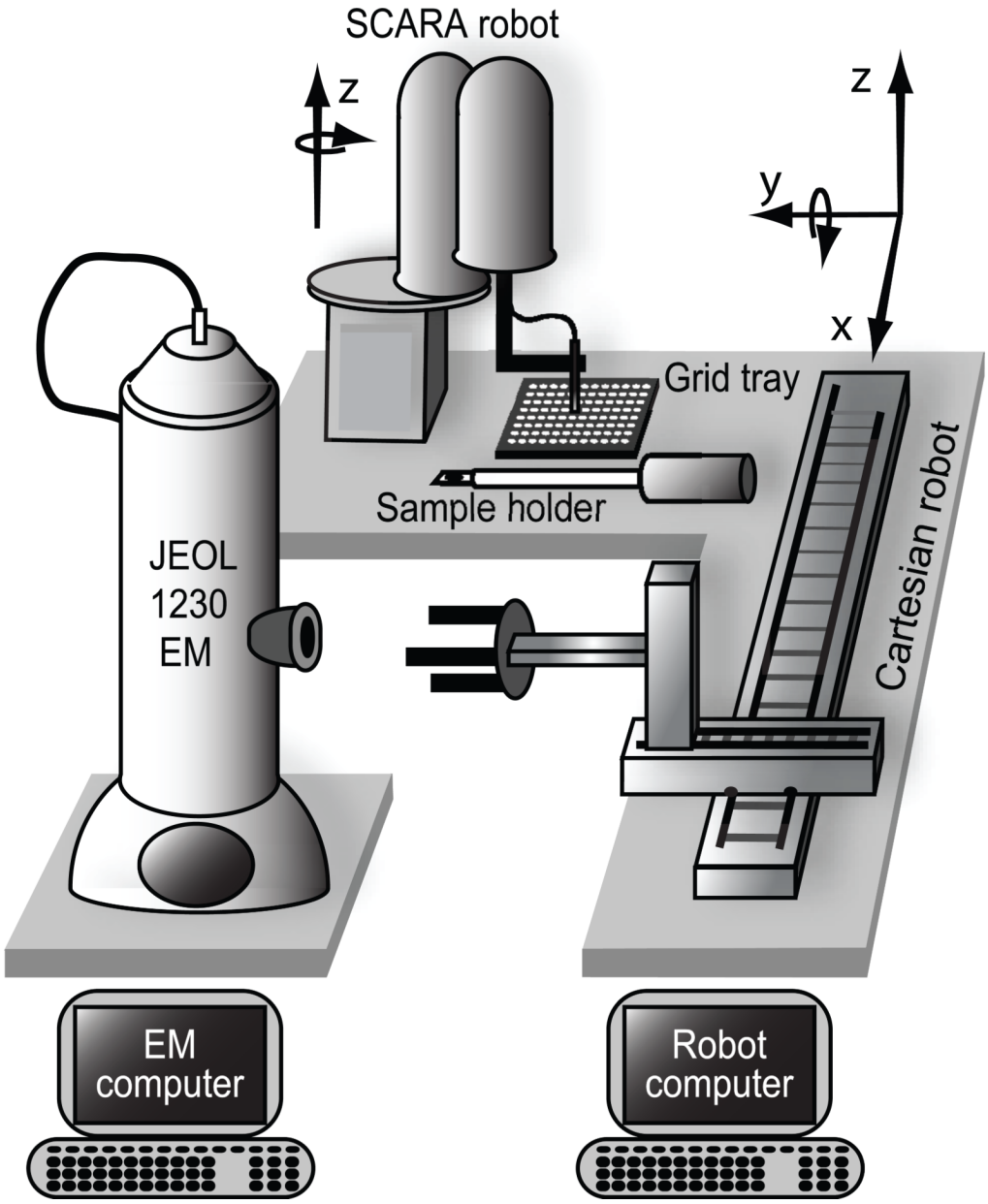

Fig. 1.

Overall layout of the robotic grid loading system. The SCARA robot is responsible for loading individual EM grids from a 96-well grid tray into the EM sample holder. The Cartesian robot is responsible for picking up this sample holder and inserting it through the goniometer on the JEOL 1230 electron microscope. Axes of movement for both robots are shown. The EM computer runs Leginon and coordinates sample loading and imaging by communicating with a database server. The Robot computer queries the database and, when requested, initiates movement of the robot to insert or remove the sample.

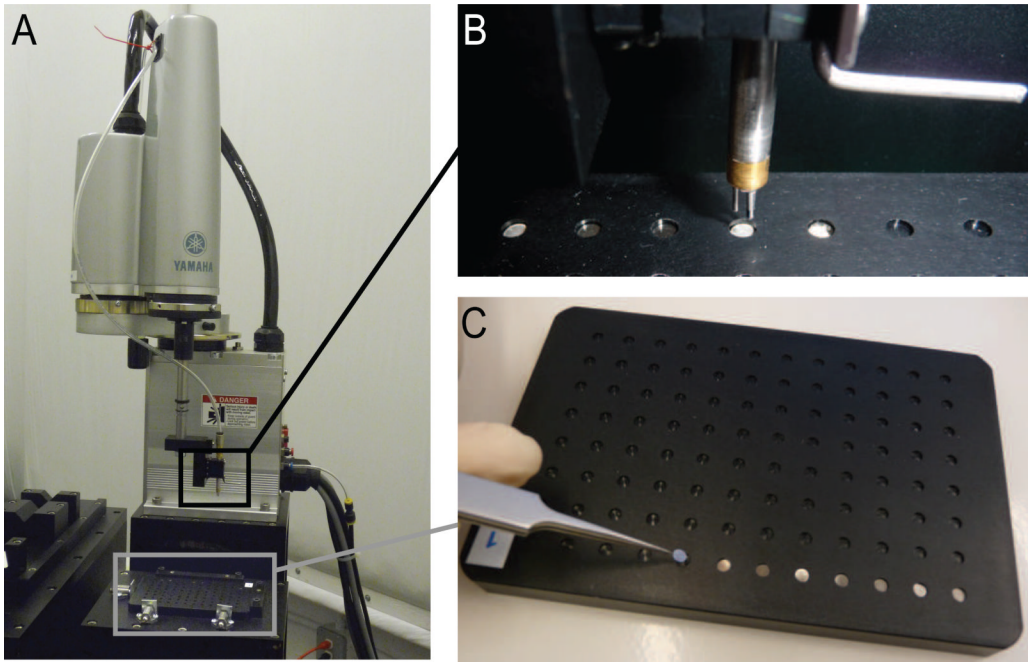

Fig. 2.

Loading EM grids. (A) A SCARA robot has been implemented for handling individual EM grids. (B) The SCARA robot is fitted with a vacuum probe to pick up grids using three nozzles positioned around the rim of the grid. (C) Grids are stored in an anodized aluminium tray with 96 wells laid out with standard SBS dimensions. Grids are transferred to this tray manually after negative staining.

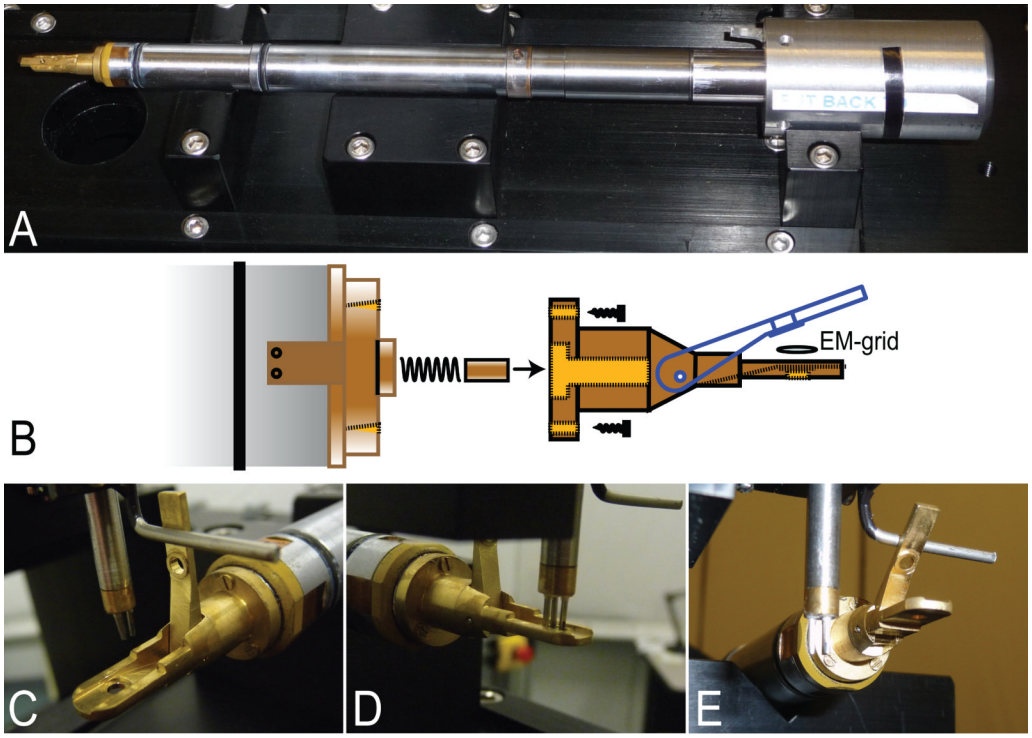

Fig. 3.

Modifications to the tip and the handle of the standard EM holder. (A) The holder is shown resting in a custom mount that serves to define its location and orientation relative to the SCARA and Cartesian robots. The original plastic holder was replaced with an aluminum handle, which was milled to be concentric with the rod. The bottom of the handle was also drilled with a hole that engages a pin on the mount (not seen) in order to maintain a defined position with respect to the robots. (B) A new tip with a spring-loaded clamp was designed for use with the SCARA robot. This exploded diagram shows how a spring pushes a piston against the eccentric hinge of the clamp. (C) An L-shaped finger mounted next to the vacuum probe raises the clamp. (D) The vacuum probe deposits the grid into the holder. (E) The L-shaped finger then lowers the clamp.

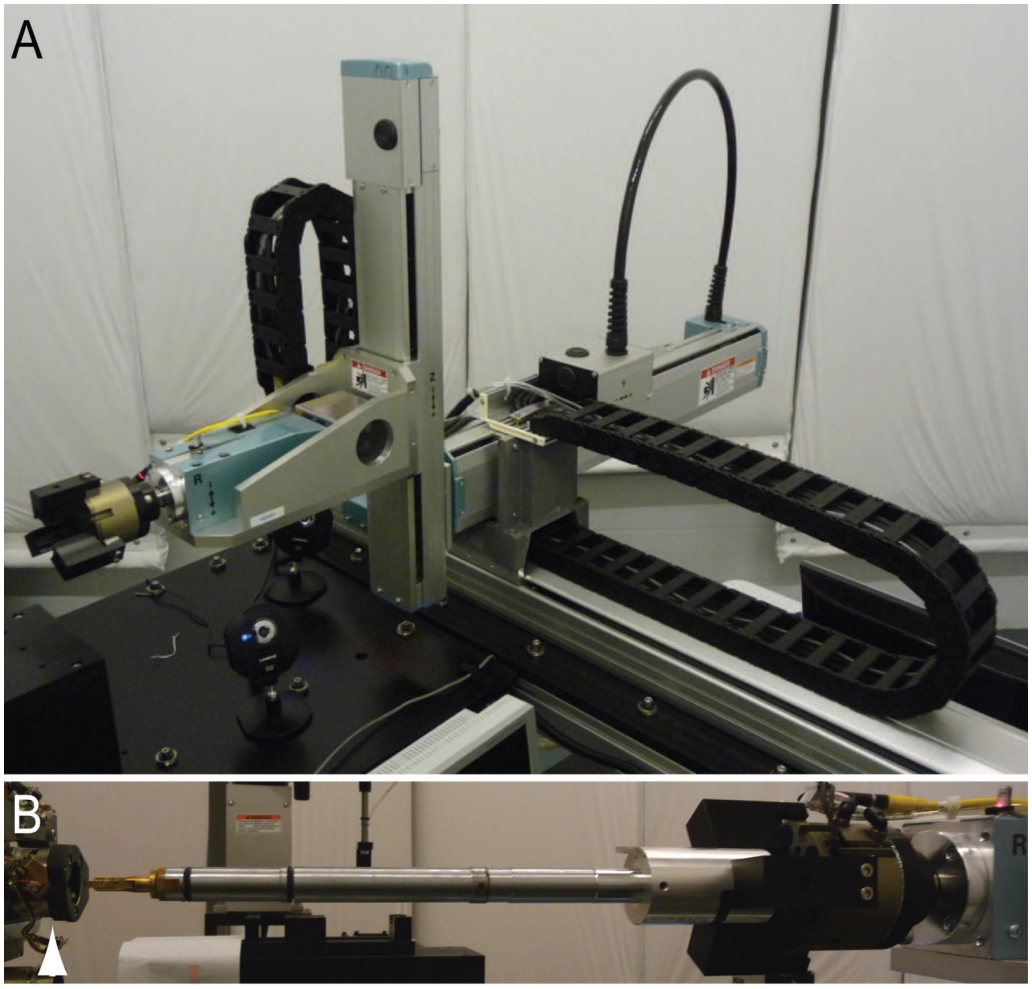

Fig. 4.

A Cartesian robot is used to move the sample holder to the microscope and insert it through the goniometer. This robot provides three orthogonal axes for linear motion and a three-fingered gripper is mounted on a rotation stage. (A) Robot prior to picking up the sample holder. (B) Robot inserting the holder into the microscope goniometer (white arrowhead on the left).

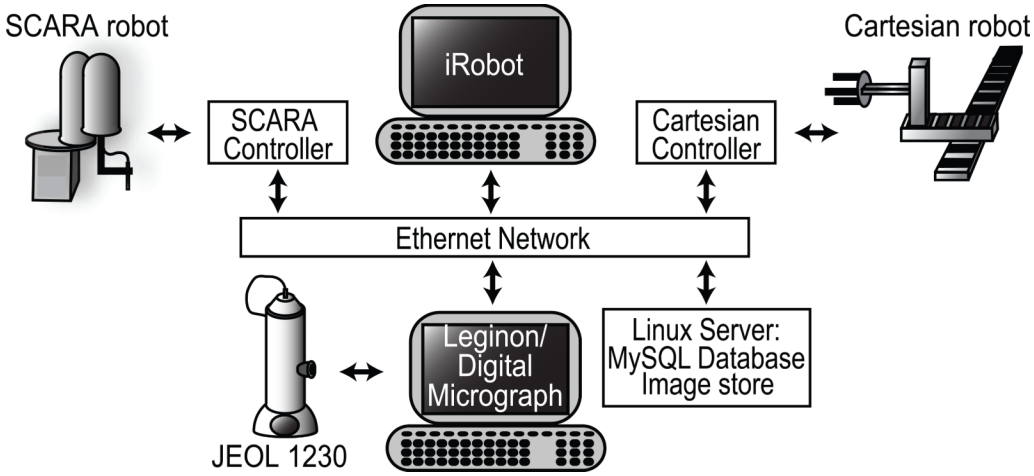

Fig. 5.

Elements of computer control connected to an Ethernet network. A Windows XP computer runs the Leginon application as well as DigitalMicrograph and communicates directly with the JEOL 1230 microscope via an RS232 serial interface. A Linux computer runs the iRobot application, which communicates with each robot via a dedicated controller. Both iRobot and Leginon communicate with second Linux computer hosting a MySQL database, which stores all the microscope calibrations and the imaging conditions as well as the images resulting from the screen.

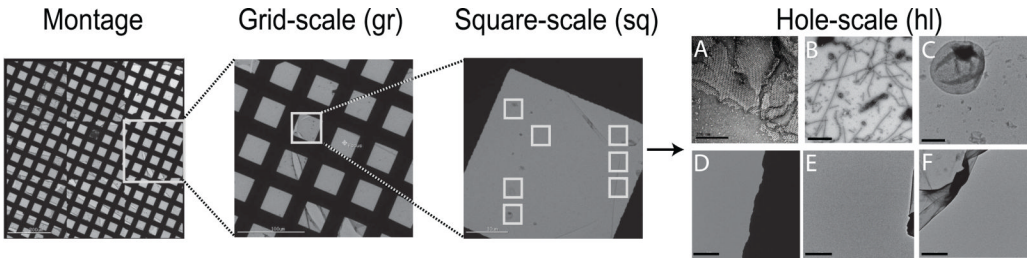

Fig. 6.

Strategy for imaging an EM grid with Leginon. As described by Cheng et al. [19], Leginon starts by recording a montage at low magnification covering a large area of the EM grid. For our application, we specified a montage containing 3x3 grid-scale images. The magnification of grid scale imaging was adjusted to include ~20 grid squares at 400 mesh. After recording the montage, Leginon evaluates individual grid squares and selects several for imaging at the square scale. We specified selection of one grid square per grid-scale image for a total of 9 per EM grid. A raster is defined at the square-scale and areas are evaluated for imaging at the hole-scale. Six examples of images at the hole scale are shown, depicting various different outcomes: 2D crystal (A), tubular crystals (B), proteoliposome (C) edge of the grid bar (D), empty grid (E) and broken carbon film (F). Scale bars correspond to 200nm in (A) and 1μm in (B-F).

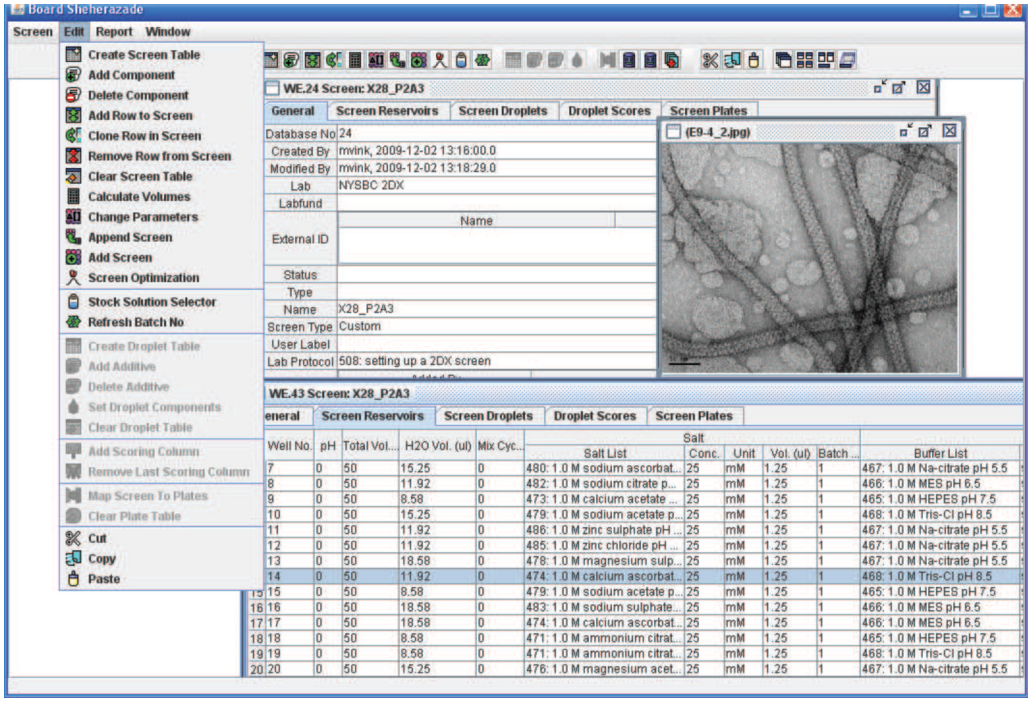

Fig. 7.

Incorporation of images into a Laboratory Information Management System. An image viewer has been added to the Sesame LIMS and images from screens have been imported into its database. This allows for integration of all information relevant to the crystallization screen, e.g., target protein sequence, conditions for expression and purification, crystallization trials, and crystallization score.